

A Novel Compact Microstrip Low-pass Filter with a Wide Rejection-Band and Sharp Roll-Off using Star-Shaped Resonator

Mohsen Hayati, Zahra Faramarzi, and Mozhgan Amiri

Electrical Engineering Department
Islamic Azad University, Faculty of Engineering, Kermanshah Branch, Kermanshah, Iran
mohsen_hayati@yahoo.com

Abstract — In this paper, a novel compact microstrip Low-Pass Filter (LPF) with a wide rejection-band and sharp roll-off using a star-shaped resonator is presented. The proposed LPF provides some significant features, such as simple structure, low insertion-loss less than 0.1 dB from DC to 2.391 GHz in the pass-band and expanded stop-band with an attenuation level better than -20 dB from 2.842 GHz up to 20.65 GHz. The transition band is 0.27 GHz from 2.57 GHz to 2.84 GHz, with corresponding attenuation levels of -3 dB and -20 dB, respectively. The filter with a -3 dB cutoff frequency of 2.57 GHz has been designed, fabricated and tested, where the measurement results are in good agreement with the simulation results. The overall size of the proposed LPF is only 11.4 mm × 13.6 mm.

Index Terms – Low-pass filter, microstrip, sharp roll-off and wide rejection band.

I. INTRODUCTION

Low-Pass Filters (LPFs) are widely used in the microwave and wireless communication systems. Recently, the design of filters in the microwave applications is based on the microstrip transmission lines incorporating with the Defected Ground Structures (DGSs), or Photonic Band Gap structures (PBG) [1]. A DGS unit is realized by etching off a simple shape defect from the ground plane that modifies the transmission line characteristics (capacitance and inductance), achieves slow-wave effect and band-stop property and causes size reduction [2-3]. PBG is done by etching a set of periodic defects in the ground plane of a microstrip structure. These PBG structures have the character of producing band gaps or stop-bands that shape the filter response.

In addition, they have the property of slowing down the propagating electromagnetic waves [4]. The PBG structures require many parameters to design of the desirable filter characteristics and it is difficult to derive an equivalent circuit model, whereas DGS needs a less parameter to design and is easy to obtain and evaluate its equivalent circuit and model [1]. However, by considering the fact that the ground plane is etched, this structure does not provide the mechanical robustness against strains [5]. Also, DGS causes the electromagnetic radiations that lead to scattering power dissipations [6]. To meet the size requirement of the modern microwave circuits, several techniques have been proposed [7]. The Invasive Weed Optimization (IWO) approach has been applied to miniaturize the Step Impedance Transmission Lines (SITL) in [8], but it doesn't have sharp roll-off response and wide stop-band. To obtain ultra-wide rejection-band, triangular and polygonal patch resonators with the meander transmission line, are implemented in [9-11], but these LPFs aren't compact enough. The Stepped Impedance Low-Pass Filter (SI-LPF) using back-to-back C-shaped and triple C-shaped units in [12] is introduced. Despite having a small physical size, it suffers from a gradual transition-band. In [13], a stepped impedance LPF using hairpin resonator with radial stubs, with intrinsic wide stop-band characteristics was employed. However, its roll-off rate is unsuitable.

In this paper, by combining the star-shaped resonator with the C-shaped stubs to suppress spurious harmonics, the designed LPF not only has a compact circuit size and sharp transition-band, but also has a wide stop-band with the attenuation level better than -20 dB. In addition, it has low insertion-loss less than 0.1 dB in the pass-band. To

reduce the circuit size of the filter, the meander transmission lines are adopted in the design of the low-pass filter.

II. FILTER DESIGN

A. Resonator design

In order to obtain a sharper roll-off, it is desirable to use a resonator structure with an elliptic function response, shown in Fig. 1. The microstrip realization of the lumped L-C element is to be approximated by use of short lengths of high and low impedance lines, illustrated in Fig. 2 [14].

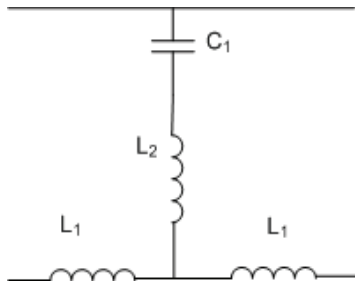


Fig. 1. A lumped element prototype low-pass resonator with an elliptic-function.

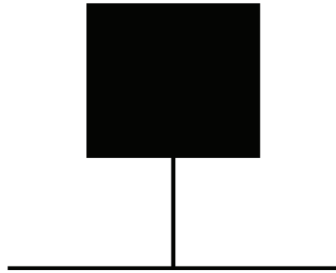


Fig. 2. Microstrip realization of the elliptic function prototype low-pass resonator.

The values of the parameters of the low and high impedance lines can be extracted using methods presented in [14]:

$$L_i = \frac{l}{2\pi f_c} Z_{oL} \sin \left(\frac{2\pi}{\lambda_{gL_i}} l_{Li} \right), \quad (1)$$

$$C_i = \frac{l}{2\pi f_c Z_{oC}} \sin \left(\frac{2\pi}{\lambda_{gC_i}} l_{Ci} \right), \quad (2)$$

where f_c is the cutoff frequency, λ_{gL} and λ_{gC} are the guided wavelength of high and low impedance lines at the cutoff frequency and Z_{oL} and Z_{oC} represent the characteristic impedance of high and low impedance lines, respectively. This resonator has a sharp transition band, but the return-loss and insertion loss in the pass-band are not suitable enough. To improve the performance of the structure, a star shaped resonator is proposed, as shown in Fig. 3. The simulation result of S-parameters of the star-shaped resonator is shown in Fig. 4.

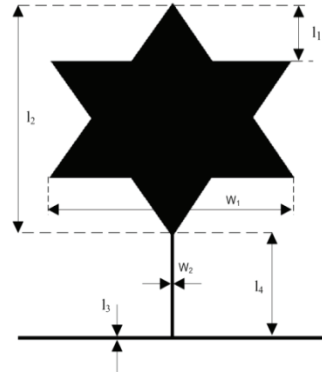


Fig. 3. Layout of the proposed star-shaped resonator.

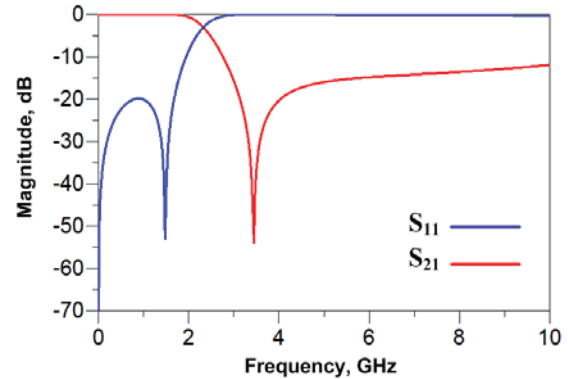


Fig. 4. S-parameters simulation of the proposed star-shaped resonator.

The accomplished comparison between frequency response of the proposed resonator and the prototype resonator shown in Fig. 5, indicates that the proposed resonator has a better pass-band response than the prototype resonator. As illustrated in Fig. 5, the star-shaped resonator has a return-loss better than -17.5 dB and an insertion-

loss better than 0.1 dB, whereas the prototype resonator has a return-loss better than -12 dB and an insertion loss better than 0.3 dB.

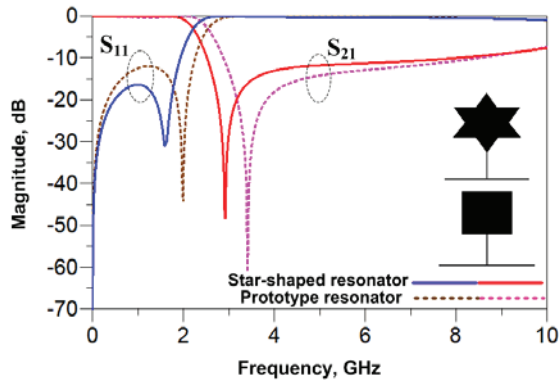


Fig. 5. Comparison between S-Parameters simulation of the prototype and proposed resonators.

As demonstrated in Fig. 6, the star-shaped resonator has a return-loss better than -17 dB in the pass-band, whereas the triangular has a return-loss better than -12 dB in the pass-band; therefore, this significant specification implies the superiority of the proposed resonator by comparison with the triangular resonator.

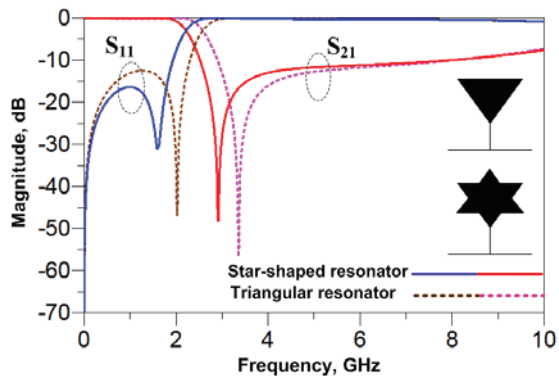


Fig. 6. Comparison between S-Parameters simulation of the triangular and proposed resonators.

Figures 7 and 8 exhibits the star-shaped resonator as a function of l_2 and l_4 , respectively. In Fig. 7, by increasing l_2 from 6.1 mm to 7.1 mm, the return-loss in the pass-band becomes better from -17 dB to -21.5 dB. By decreasing l_2 from 6.1 mm to 5.1 mm, the attenuation level of the return-loss in

the pass-band becomes worse from -17 dB to -13.9 dB. As illustrated in Fig. 8, due to reducing the physical size of the resonator by decreasing l_4 from 2.7 mm to 1.7 mm, the transmission zero near the pass-band changes from 2.92 GHz to 3.476 GHz, which leads to a gradual transition-band. While by increasing l_4 from 2.7 mm to 3.7 mm, the mentioned transmission zero changes from 2.92 GHz to 2.559 GHz, which results in a sharper transition-band. Therefore, these parameters are significant to optimize some attributes of the resonator.

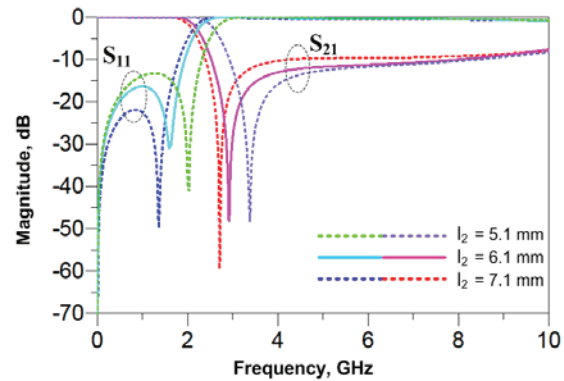


Fig. 7. S-parameters simulation of the proposed resonator as a function of l_2 .

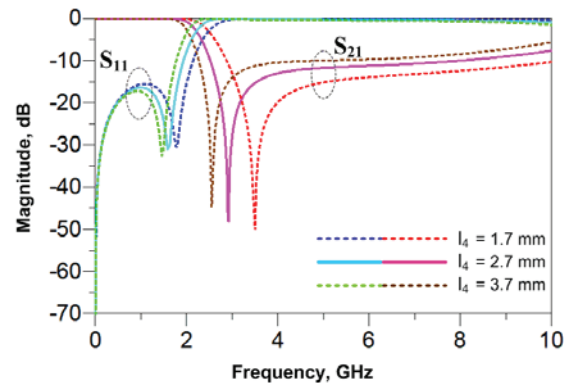


Fig. 8. S-parameters simulation of the proposed resonator as a function of l_4 .

B. Filter design

To eliminate the high frequency harmonics and obtain a wider stop-band region, it is needed to add a suppressing cell to the proposed resonator. Figure 9 exhibits the layout and frequency response of two C-shaped suppressor

cells. As shown in Fig. 9, these stubs result in extra finite transmission zero within the stop-band that suppress the harmonics and also extends the stop-band. As indicated in Fig. 10, the asymmetrical C-shaped stubs have the better pass-band response due to its -50 dB return-loss, in comparison with symmetrical C-shaped stubs, which has -21 dB return-loss. Therefore, using these asymmetrical C-shaped stubs, the return-loss for the final structure of the LPF will be better.

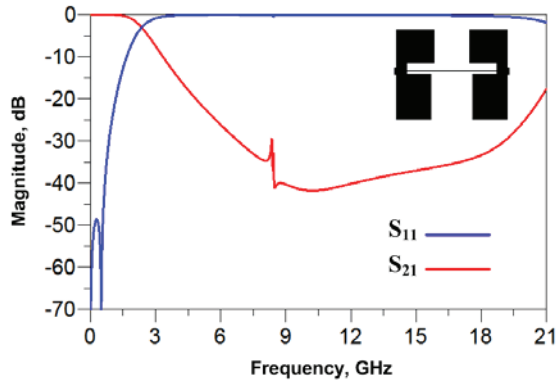


Fig. 9. Layout and S-parameter simulation of C-shaped stubs.

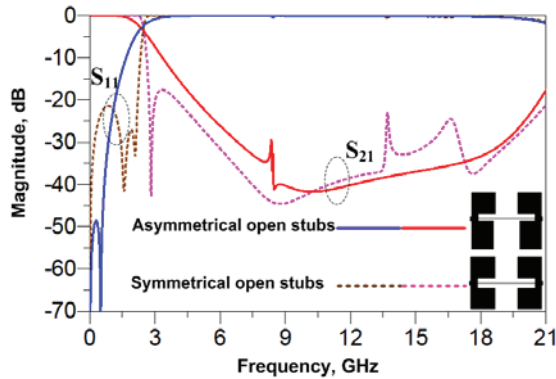


Fig. 10. Comparison between S-Parameters of the symmetrical open stubs and the C-shaped stubs.

The layout of the proposed LPF is shown in Fig. 11, in which the meander transmission lines are used to reduce the physical size of the proposed LPF. The input/output ports are matched to 50Ω , using two stubs with dimensions of $L_f=2.3$ mm and $W_f=1.5$ mm. The dimensions of the proposed LPF are as specified in Table 1.

Table 1: Dimensions of proposed LPF (mm)

$l_1=1.5$	$l_2=6.1$	$l_3=0.1$	$l_4=2.7$
$l_5=3.3$	$l_6=0.7$	$l_7=4.5$	$l_8=0.2$
$l_9=0.7$	$l_{10}=0.5$	$W_1=7$	$W_2=0.1$
$W_3=3.8$	$W_4=3.8$	$W_5=3.5$	$W_6=1.1$

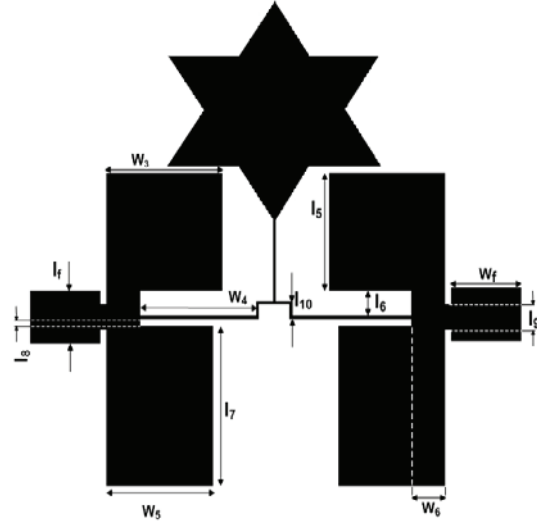


Fig. 11. Layout of proposed LPF.

III. SIMULATION AND MEASUREMENT

The photograph of the fabricated proposed LPF and also measurement and simulation results, are shown in Figs. 12 and 13, respectively. The EM simulation of the LPF is performed by the ADS software. The suggested LPF is fabricated on a RT/Duroid 5880 substrate with the dielectric constant of 2.2, loss-tangent of 0.0009 and height of 0.508 mm.

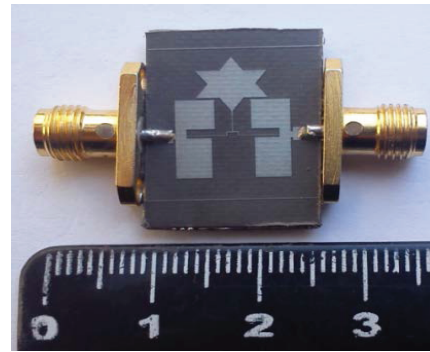


Fig. 12. Photograph of the fabricated LPF.

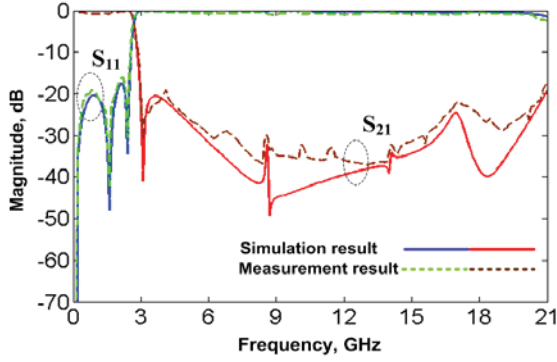


Fig. 13. Measured and simulated S-parameter of the proposed filter.

The measurement is performed by an Agilent network analyzer. As indicated in Fig. 13, there is a good agreement between the simulation and measurement results. The maximum variation of the group delay of the proposed LPF in the 93% of the pass-band region is 0.475 ns; which is a very small amount, nearby an ideal point for a LPF, as illustrated in Fig. 14. The proposed LPF with -3 dB cutoff frequency of 2.57 GHz has the insertion loss less than 0.1 dB from DC to 2.391 GHz (which is about 93% of the pass-band bandwidth). The stop-band bandwidth is 17.81 GHz (from 2.84 GHz to 20.65 GHz), with the attenuation level better than -20.5 dB; thus, the expanded stop-band is 6.93 times of -3 dB cutoff frequency. The transition-band between -3 dB and -20 dB is about 0.27 GHz. In addition, the overall size of the LPF is only 11.4 mm × 13.6 mm.

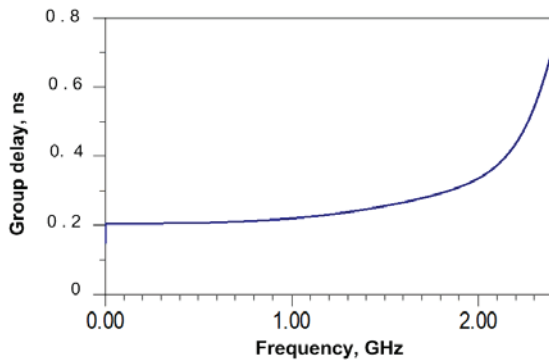


Fig. 14. Group-delay of the proposed LPF.

The performance of the proposed LPF in comparison with other published works is summarized in Table 2. Where ζ is the roll-off rate

that is used to evaluate the roll-off sharpness, which is defined as [15]:

$$\zeta = \frac{\alpha_{max} - \alpha_{min}}{f_s - f_c}, \quad (3)$$

where α_{max} is the -20 dB attenuation point, α_{min} is the -3 dB attenuation point, f_s is the -20 dB stop-band frequency and f_c is the -3 dB cutoff frequency.

The Relative Stop-band Bandwidth (RSB) is given by [15]:

$$RSB = \frac{stopband(-20dB)}{stopband\ center\ frequency}. \quad (4)$$

The Normalized Circuit Size (NCS) is applied to measure the degree of the miniaturization of different filters and formulated as [15]:

$$NCS = \frac{physical\ size\ (length \times\ width)}{\lambda_g^2}, \quad (5)$$

where λ_g is the guided wavelength at -3 dB cutoff frequency.

The Suppressing Factor (SF) is related to the suppression in the stop-band and calculated as [15]:

$$SF = \frac{Rejection\ level}{10}. \quad (6)$$

The Architecture Factor (AF) can be identified as the circuit complexity factor, which is signed as 1 when the design is 2D and as 2 when the design is 3D. Finally, the Figure-of-Merit (FOM) is defined as [15]:

$$FOM = \frac{\zeta \times RSB \times SF}{NCS \times AF}. \quad (7)$$

Table 2: Performance comparison of the proposed LPF with other published works

Ref.	ζ (dB/GHz)	RSB	NCS (λ_g^2)	FOM
[1]	34.48	1.22	0.096	876
[5]	43.58	1.67	0.029	5020
[6]	27.40	0.68	0.009	4140
[9]	24.28	1.65	0.010	6009
[10]	23.53	1.55	0.007	7815
[11]	25.00	1.51	0.008	8022
[12]	28.33	1.03	0.012	4863
[13]	22.66	1.25	0.006	7081
This work	62.35	1.52	0.021	9252

According to Table 2, the proposed low-pass filter has a good RSB and also has the highest roll-off rate and FOM among the published works.

IV. CONCLUSION

In this paper, a LPF using the star-shaped resonator combined with C-shaped suppressing cells is designed, fabricated and measured. This structure leads to a compact size, sharp roll-off characteristic and an expanded stop-band bandwidth, as well as good insertion loss and return-loss in both stop-band and pass-band region. Also, because of having a simple structure, the fabrication process is so convenient. The proposed structure with such a high performance can be applied in modern high frequency communication systems as an efficient and merit LPF.

ACKNOWLEDGMENT

The authors would like to thank the Islamic Azad University, Kermanshah Branch, for their financial support of this research project.

REFERENCES

- [1] A. S. Mohra, "Microstrip low pass filter with wideband rejection using opened circuit stubs and z-slots defected ground structures," *Microwave and Optical Technology Letters*, vol. 53, no. 4, pp. 811-815, April 2011.
- [2] M. Al-Sharkawy, A. Boutejdar, F. Alhefnawi, and O. Luxor, "Improvement of compactness of low-pass/band-pass filter using a new electromagnetic coupled crescent defected ground structure resonators," *Applied Computational Electromagnetics Society Journal*, vol. 25, no. 7, pp. 570-577, July 2010.
- [3] M. Challal, A. Boutejdar, M. Dehmas, A. Azrar, and A. Omar, "Compact microstrip low-pass filter design with ultra-wide reject and using a novel quarter-circle DGS shape," *Applied Computational Electromagnetics Society Journal*, vol. 27, no. 10, October 2012.
- [4] G. E. Al-Omar, S. F. Mahmoud, and A. S. Al-Zayed, "Low-pass and band-pass filter designs based on DGS with complementary split ring resonators," *Applied Computational Electromagnetics Society Journal*, vol. 26, no. 11, November 2011.
- [5] Y. Yousefzadeh and M. Hayati, "Compact low-pass filter with wide stopband using a tapered microstrip resonator cell," *Microwave Journal*, vol. 55, no. 3, pp. 122-128, March 2012.
- [6] M. H. Yang, J. Xu, Q. Zhao, L. Peng, and G. P. Li, "Compact broad stop-band low-pass filters using sirs-loaded circular hairpin resonators," *Progress In Electromagnetics Research*, vol. 102, pp. 95-106, 2010.
- [7] A. Adinehvand and A. Lotfi, "Compact low-pass filter with wide stop-band using open stubs-loaded spiral microstrip resonant cell," *Applied Computational Electromagnetics Society Journal*, vol. 28, no. 1, January 2013.
- [8] H. R. Khakzad, S. H. Sedighy, and M. K. Amirhosseini, "Design of compact SITLs low-pass filter by using invasive weed optimization (IWO) technique," *Applied Computational Electromagnetics Society Journal*, vol. 28, no. 3, March 2013.
- [9] J. Wang, H. Cui, and G. Zhang, "Design of compact microstrip low-pass filter with ultra-wide stop band," *Electronics Letters*, vol. 48, no. 14, pp. 854-856, July 2012.
- [10] H. Cui, J. Wang, and G. Zhang, "Design of microstrip low-pass filter with compact size and ultra-wide stop-band," *Electronics Letters*, vol. 48, no. 14, pp. 856-857, July 2012.
- [11] L. Ge, J. P. Wang, and Y. X. Guo, "Compact microstrip low-pass filter with ultra-wide stop band," *Electronics Letters*, vol. 46, no. 10, pp. 689-691, May 2010.
- [12] J. Y. Wu, Y. H. Tseng, and W. H. Tu, "Design of compact low-pass filter with ultra-wide stop band using thin slots," *Progress In Electromagnetics Research C*, vol. 31, pp. 137-151, 2012.
- [13] X. B. Wei, P. Wang, M. Q. Liu, and Y. Shi, "Compact wide stop-band low-pass filter using stepped impedance hairpin resonator with radial stubs," *Electronics Letters*, vol. 47, no. 15, pp. 862-863, July 2011.
- [14] J. S. Hong and M. J. Lancaster, "Microstrip filters for RF/microwave applications," *John Wiley & Sons, Inc.*, New York, 2001.
- [15] M. Hayati, F. Shama, and H. Abbasi, "Compact microstrip low-pass filter with wide stop-band and sharp roll off using tapered resonator," *International Journal of Electronics*, vol. 100, no. 12, pp. 1751-1759, 2013.



Mohsen Hayati received his B.E degree in Electronics and Communication Engineering from Nagarjuna University, India in 1985 and his M.E. and Ph.D. degrees in Electronics Engineering from Delhi University, Delhi, India in 1987 and 1992, respectively. He joined the Electrical Engineering Department at Razi

University, Kermanshah, Iran as an Assistant Professor in 1993. At present, he is an Associate Professor with the Electrical Engineering Department at Razi University. He has published more than 135 papers in international and domestic journals and conferences. His current research interests include microwave and millimeter wave devices and circuits, application of computational intelligence, artificial neural networks, fuzzy systems, neuro-fuzzy systems, electronic circuit synthesis and modeling and simulations.



Zahra Faramarzi received her B.E. and M.E. degrees in Electronics Engineering from Razi University, Kermanshah, Iran in 2005 and 2013, respectively. Her current research interests include design of RF circuits and MMIC.



MMIC.

Mozghan Amiri received her B.E. and M.E. degrees in Electronics Engineering from Razi University, Kermanshah, Iran in 2005 and 2013, respectively. Her current research interests include RF electronics microwave circuit design and modeling RFIC and